Multiobjective Control of a Four-Link Flexible Manipulator: A Robust H_∞ Approach

Zidong Wang, Hanqing Zeng, Daniel W. C. Ho, and H. Unbehauen

***Abstract*—This paper presents a new approach to robust H_∞ control of a real multilink flexible manipulator via regional pole assignment. We first show that the manipulator system can be approximated by a linear continuous uncertain model with exogenous disturbance input. The uncertainty occurring in an operating space is assumed to be norm-bounded and enter into both the system and control matrices. Then, a multiobjective simultaneous realization problem is studied. The purpose of this problem is to design a state feedback controller such that, for all admissible parameter uncertainties, the closed-loop system simultaneously satisfies both the prespecified H_∞ norm constraint on the transfer function from the disturbance input to the system output and the prespecified circular pole constraint on the closed-loop system matrix. A new algebraic parameterized approach is developed to characterize the existence conditions as well as the analytical expression of the desired controllers. Third, by comparing with the traditional linear quadratic regulator (LQR) control method in the sense of robustness and tracking precision, we provide both the simulation and experimental results to demonstrate the effectiveness and advantages of the proposed approach.**

***Index Terms*—Flexible structures, H_∞ control, multilink manipulators, regional pole assignment, robust control.**

I. Introduction

ROBOT manipulators are widely applied in industrial practice. Conventional rigid manipulators are often built to be heavy and bulky for high structural stiffness. The advantage of rigid manipulators lies in that they can be easily controlled. But some drawbacks, such as high power consumption, low motion speed, actuators with high capacity, and low payload ratio, may appear. To remedy these drawbacks, the manipulator can be made of lightweight materials. As opposed to the bulky structure, lightweight structures can improve the performance of manipulators with typically low payload-to-arm weight ratio and enable the manipulators to achieve fast and dexterous motion. These energy efficient manipulators are of special interest in many application fields such as space robotic systems and vehicles. However, the lightweight structure will bring new problems. First, the structural flexibility will lead to a high degree of elastic vibration especially during the high-velocity maneuver of the manipulators. Also, some nonlinear phenomenon such as joint friction will play a more important role in the dynamics of the lightweight manipulators. For example, the joint friction results in a very complicated dynamics especially when the lightweight manipulator is operating at low velocities. Furthermore, the dynamic equations of motion are nonlinear and of large dimensions. These problems aggravate the difficulty of the modeling, identification, and control of lightweight manipulators.

Multilink lightweight manipulators present even more complex problems for control. It is not easy to obtain a high accuracy dynamic model or black-box model of multilink lightweight manipulators for the purpose of control design. On the other hand, the control system of lightweight manipulators belongs to the class of mechanical systems, where the number of controlled variables is strictly less than the number of mechanical degrees of freedom, since the flexible links are subject to deflection and vibration. Furthermore, the linear effects of flexibility are not separated from typical nonlinear effects of multibody rigid dynamics. For a high-performance lightweight manipulator, the task is to track a smooth trajectory of motion. This can be assigned at the joint level, as if the manipulator were rigid. Provided that the link deformation is kept limited, satisfactory results may be obtained also at the end-effector level.

Motion control of flexible manipulators has recently attracted a great deal of interest from many researchers. With the advances in modern control theories, many control schemes have been successfully proposed to tackle the modeling and control problems of flexible manipulators. For example, the linear control approaches, such as linear quadratic regulator (LQR) and acceleration feedback control methods, have been used for the controller design in [14], [21]. The nonlinear control methods, such as those using computed torque, inverse dynamics, and feedback linearization, have been proposed in [1], [3], and [15], respectively. More recently, the robust control approaches, such as H_∞ design, robust pole assignment, and d-stability constraints, have received considerable attention (see, e.g., [5], [16], and [20]). It is noticeable that most of the papers mentioned above have only dealt with the control problem of single link flexible manipulators. Thus, the primary aim of this paper is to develop a new approach to designing robust H_∞ feedback controllers, and then show its real-time application in the control of a *multilink* flexible manipulator.

Although the robust H_∞ design is mainly related to robust stability and frequency-domain performance specifications, it deals little with the transient behavior which is also important in the control of multilink flexible manipulators. As is well known, the pole location is directly associated with the dy-

Manuscript received October 9, 2000. Manuscript received in final form July 10, 2002. Recommended by Associate Editor E. G. Collins, Jr. The work of Z. Wang was supported in part by the City University of Hong Kong under RGC Grant with CityU 1138/01P, the University of Kaiserslautern, Germany, and the Alexander von Humboldt Foundation, Germany. The work of H. Zeng was supported by the German Academic Exchange Service (DAAD).

Z. Wang is with the Department of Information Systems and Computing, Brunel University, Uxbridge, Middlesex UB8 3PH, U.K. (e-mail: Zidong.Wang@brunel.ac.uk).

H. Zeng is with Nortel Networks, Lapean, ON K2H 8E9, Canada.

D. W. C. Ho is with the Department of Mathematics, City University of Hong Kong, Kowloon, Hong Kong.

H. Unbehauen is with the Control Engineering Laboratory, Department of Electrical Engineering and Information Science, Ruhr-University Bochum, D-44780 Bochum, Germany.

Digital Object Identifier 10.1109/TCST.2002.804132

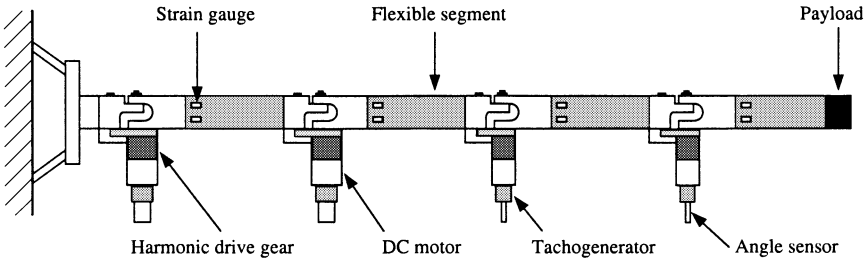

Fig. 1. Schematic structure of the multilink flexible manipulator.

namical characteristics of linear time-invariant systems such as damping rates, natural, and damped natural frequencies, and therefore, the problem of pole assignment in linear system theory has been discussed by many authors and solved in various ways (see [12], [13], and references therein). On the other hand, locations of poles vary and cannot be fixed due to parameter uncertainties that originate from various sources, such as variation of operating points, identification errors of parameters, etc. Hence, placing all poles of the overall system in a desired region rather than choosing an exact assignment may be satisfactory in the control of multilink flexible manipulators. A well-known desired region for continuous systems is a disc $D(-q, r)$ in the left-half complex plane with the center at $-q + j0(q > 0)$ and radius $r(r < q)$. We say a linear time-invariant system is *d-stable* if the corresponding system poles are all located inside a disc.

In the past decade, a large amount of interest has been given to the problem of controller design for assigning all closed-loop poles within a desired circular region (see, e.g., [11] and [19]). Furthermore, the robust circular pole-assignment (i.e., robust d-stabilization) problem for systems with parameter perturbations has recently been well studied (see, e.g., [7], [8], [17], [22], and [23], where the H_∞ index has unfortunately not been included).

It should be pointed out that, very recently, in [5], the discrete-time robust d-stabilization theory developed in [7] and [8] has been successfully applied in the real-time control of a manipulator. However, in the event of feedback control for an inherently time-continuous system in terms of a discrete-time "equivalent," the question of sampling is not trivial, since the very small sampling period which is naturally required will result in computational difficulties. Moreover, the parameters in the discrete-time model usually do not correspond to the physical meanings and this brings difficulties in parameter identification. Therefore, in this paper, we cope with the problem of designing robust d-stability controller for a real *multilink* flexible manipulator in a continuous-time setting. Different from the existing results, in addition to the robustness and transient behavior, we further enforce the disturbance rejection property onto the feedback system so that the better performance of the controlled manipulator can be achieved. The H_∞ norm of the transfer function from the disturbance input to the system output is guaranteed to be less than an expected upper bound. We illustrate the relevant advantage through both simulation and experiments by comparing with some traditional control methods.

The organization of this paper is as follows. In Section II, we first give a description of the physical plant, and use a continuous uncertain model with exogenous disturbance input to approximate the manipulator system. The robust H_∞ control problem is then formulated. Section III presents the design procedure of robust H_∞ state feedback controllers with d-stability constraints. In particular, we develop a new algebraic parameterized approach and establish both the existence conditions and the analytical expression of desired controllers. Simulation and experimental results are given in Section IV to demonstrate the effectiveness and advantages of the proposed approach. Finally, the conclusions are included in Section V.

The notation is standard. Throughout this paper, $\mathbb{R}^n$ and $\mathbb{R}^{n\times m}$ denote, respectively, the n-dimensional Euclidean space and the set of all $n \times m$ real matrices. The superscript "T" denotes matrix transposition and the notation $X \geq Y$ (respectively, $X > Y$) where X and Y are symmetric matrices, means that $X - Y$ is positive semidefinite (respectively, positive definite). I_n stands for the $n \times n$ identity matrix.

II. Problem Description

A. Description of the Plant

The plant is a four-link flexible manipulator which was developed at the Control Engineering Laboratory, Department of Electrical Engineering and Information Sciences, Ruhr-University Bochum, Bochum, Germany [6]. Fig. 1 shows the schematic structure of this manipulator.

The whole robot control system consists of a host computer, the transputer network, the real-time measurement system (RTMS) and a planar four-link lightweight manipulator. The host computer serves as the man–machine interface of the plant. A special software called TROB [6] was developed by using C++. This software environment can be used for manipulating the robot experiments. The transputer network consists of seven transputers and two DSPs. It has been designed to allow the implementation of both the decentral and multiinput–multioutput (MIMO) controller.

The RTMS is a VPORT 50-based data acquisition system. The operating system of RTMS can coordinate any measurement into the transputer network. The program for operating the whole plant is object-oriented. The joints are driven by dc motors with harmonic drive gears [10]. Two large motors (HDSA20) are used for the first two joints with electromagnetic break and two small motors (HDSH14) for the other two joints

TABLE I
TECHNICAL SPECIFICATIONS OF THE DC MOTORS

	Joint 1	Joint 2	Joint 3	Joint 4
Type	HDSA 20	HDSA 20	HDSH 14	HDSH 14
Rated voltage	24 V	24 V	24 V	24 V
Rated power	94 W	94 W	18.5 W	18.5 W
Rated torque	30 Nm	30 Nm	5.9 Nm	5.9 Nm
Rated current	8.5 A	8.5 A	1.8 A	1.8 A
Torque gain	4.5 Nm/A	4.5 Nm/A	5.65 Nm/A	5.65 Nm/A
Gear reduction	100	100	101	101
Inertia (motor+gear)	1.06 kg·m^2	1.06 kg·m^2	0.081 kg·m^2	0.081 kg·m^2

TABLE II
STRUCTURAL SPECIFICATION OF THE MANIPULATOR

Material of the links (1 – 4):	Aluminum alloy
Length of the links (1 – 4):	0.6 m
Length of the flexible part of the links (1 – 4):	0.24 m
Width of the flexible part of the links (1 – 4):	0.017 m
Height of the flexible part of the links (1 – 4):	0.1 m
Density of the links (1 – 4):	2690 kg/m^3
Flexural rigidity of the links (1 – 4):	1050 Nm^2
Masses of the joint 1,2:	9.16 kg
Masses of the joint 3,4:	6.14 kg
Payload of the manipulator:	0 till 5 kg

without break system respectively. The technical specifications of the dc motors are shown in Table I.

The link segments are made of aluminum, and the elastic vibrations of the links are measured by strain gauges. Table II shows the structural specification of the manipulator.

The input signal is the control voltage which is the output of the controller. The output signals include the angle output of the joint, the elastic vibration of the link, the signals for the emergency brake, and the current in the armature of the dc motor.

More details concerning the technical description of the plant and related software are given in [6].

B. Dynamic Modeling

The physical modeling of manipulators can be classified into two categories: kinematic and dynamic modeling. Both the kinematic and dynamic modeling rely on an accurate knowledge of a number of constant parameters characterizing the mechanical structure, such as link lengths, masses, and inertial properties.

The kinematic modeling of a manipulator concerns the description of the motion of the manipulator with respect to a fixed reference frame by ignoring the forces and moments that cause this motion of its structure. The kinematic method is usually considered in terms of forward kinematics, inverse kinematics, and velocity kinematics. On the other hand, the dynamic modeling aims at the derivation of the motion equations of the manipulator as a function of the forces and moments acting on it. Many methods are available in the robotics literature (see, for example, [4]). Two kinds of equations are mainly used to derive the dynamic model, namely, the Lagrange's equation and the Newton–Euler's equation. Both equations lead to exactly the same final answers of the manipulator dynamics.

In this paper, we adopt the dynamic modeling for the multilink lightweight manipulators, which is inherited from that of the rigid manipulators. The difficulty encountered in this modeling can be traced to the distributed nature of the system, for example, the structural deformation. The motion of such manipulators is described by partial differential equations rather than ordinary differential equations. The search for solutions is even further hampered by the fact that the solutions depend strongly on the boundary conditions. While the boundary conditions vary rapidly with time due to the varying configuration of the lightweight manipulator, this property makes it nearly impossible to find closed-form solutions.

On the basis of the above discussion, we will follow the standard Lagrange formulation for the rigid-link case, to derive the dynamic equations of motion of a planar n-link flexible manipulator. To constitute a set of generalized coordinates of the system, it is necessary to introduce not only the n joint angles $\theta = [\theta_1, \ldots, \theta_n]^T$, but also the elastic modes $\delta = [\delta_{11}, \ldots, \delta_{ij}, \ldots, \delta_{nm_n}]^T$ where $i = 1, \ldots, n$ and $j = 1, \ldots, m_i$. The following assumption is made on the flexible links.

Assumption 1: The number of significant modes m_i is sufficient to obtain a good approximation of the elastic deformation of the ith link.

Based on Assumption 1, the elastic deformation $w(x, t)$ of the ith link at a distance x from the joint can be expressed as the sum of appropriate basis functions $\phi_{ij}(x)$ multiplied by the modal coordinates δ_{ij}, that is

$$w_i(x, t) = \sum_{j=1}^{m_i} \phi_{ij}(x)\, \delta_{ij}(t). \tag{1}$$

If the trajectories are assigned at the joint level, the end-effector position of link i can then be approximately described by using the pseudojoint angle as

$$y_i(t) = \theta_i + w_i(x, t)/l_i. \tag{2}$$

Now we define the generalized coordinates of the system q as follows:

$$q = [\theta_1 \cdots \theta_n\, \delta_{11} \cdots \delta_{1m_1} \cdots \delta_{n1} \cdots \delta_{nm_n}]^T \tag{3}$$

and then the dynamics of n-link flexible manipulators can be derived by using the Lagrangian approach, which leads to

$$M(q)\ddot{q} + C(q, \dot{q})\dot{q} + K_d q = u \tag{4}$$

where $M(q)$ is the positive-definite symmetric inertia matrix of the manipulator, $C(q, \dot{q})\dot{q}$ includes the coriolis and centrifugal moments, $K_d q$ is the effect of structural deformation, and u is the generalized vector of joint moments defined by

$$u = [u_1 \cdots u_n\, 0 \cdots 0]^T. \tag{5}$$

Defining a new state vector $x = [q^T\, \dot{q}^T]^T$ and differentiating x, we have

$$\dot{x} = \begin{bmatrix} \dot{q} \\ \ddot{q} \end{bmatrix} = \begin{bmatrix} 0 & I \\ -M^{-1}K_d & -M^{-1}C \end{bmatrix} \begin{bmatrix} q \\ \dot{q} \end{bmatrix} + \begin{bmatrix} 0 \\ M^{-1} \end{bmatrix} u. \tag{6}$$

and therefore the dynamic model of the multilink flexible manipulator can be described by

$$\dot{x}(t) = A(x)x(t) + B(x)u(t) \tag{7}$$

where the nonlinear system matrices $A(x)$, $B(x)$ are the function of the state vector $x(t)$.

In this paper, we linearize the nonlinear system (7) at a operating point. Then, consider the linearized system with both parameter perturbations of system dynamics and additive disturbance term as follows:

$$\begin{aligned}\dot{x}(t) &= (A + \Delta A)x(t) + (B + \Delta B)u(t) + Dw(t)\\ y(t) &= Ex(t)\end{aligned} \tag{8}$$

where $x(t) \in \mathbb{R}^{n_x}$, $u(t) \in \mathbb{R}^{n_u}$, and $w(t) \in \mathbb{R}^{n_w}$ are the system state, the control input and the disturbance input, respectively. $y(t) \in \mathbb{R}^{n_y}$ represents the system output which is the vector of pseudo joint angles. A, B, D, and E are constant matrices with appropriate dimensions that describe the nominal system, and ΔA, ΔB are real-valued matrix functions representing the time-invariant parameter uncertainty. For the given operating point of an operating space, the parameter uncertainties ΔA, ΔB can be constructed to approximate the major linearization errors of the system (6). These parameter uncertainties can then be considered here to be norm-bounded and of the form

$$[\Delta A\ \Delta B] = SF[N_1\ N_2] \tag{9}$$

where S, N_1, N_2, and $(N_2^T N_2 > 0)$ are known real constant matrices with appropriate dimensions, and F is an uncertain constant matrix satisfying

$$F^T F \le I. \tag{10}$$

The term $w(t)$ can be used to describe the additive disturbance, for examples, the noise, the nonlinear terms in the dynamics of manipulators, the loads varying for different tasks, etc. To guarantee the admissible disturbance attenuation level in the sequel, the H_∞ requirements will be considered in this paper.

Remark 1: The parameter uncertainty structure as in (9) and (10) has been widely used in the problems of robust control and robust filtering of uncertain systems (see, e.g., [7], [8], [17], [23], and the references therein). Many practical systems possess parameter uncertainties which can be either exactly modeled or overbounded by (10). Moreover, unlike the existing results, we use the "disturbance term" in the model to account for the influence from the operating environment, and the H_∞ requirement is introduced to reduce the possible affection from the "disturbance input."

C. Control Problem Formulation

Applying the state feedback control law

$$u(t) = Kx(t) \tag{11}$$

to the system (8), we can obtain the resulting closed-loop system as follows:

$$\dot{x}(t) = (A_c + \Delta A_c)x(t) + Dw(t), \qquad y(t) = Ex(t) \tag{12}$$

where $A_c = A + BK$, $\Delta A_c = SF(N_1 + N_2 K)$. For the system (12), the closed-loop transfer function $H(s)$ from disturbance input $w(t)$ to output $y(t)$ can be written as

$$H(s) = E[sI - (A_c + \Delta A_c)]^{-1} D. \tag{13}$$

Consider a circular region $D(-q, r)$ in the left-half complex plane with the center at $-q + j0\,(q > 0)$ and the radius $r\,(r < q)$ for continuous systems. Now, the major aim of the robust H_∞-norm circular pole placement control (RHCPPC) problem is to design the state feedback gain K such that, *for all admissible uncertainties satisfying* (9), (10), the following performance criteria are simultaneously achieved

C1: The closed-loop poles are constrained to lie within the specified disc $D(-q, r)$, i.e., $\sigma(A_c + \Delta A_c) \subset D(-q, r)$, where $-q$ is the center on the real axis and r is the radius of this disc.

C2: The H_∞ norm of the disturbance transfer matrix $H(s)$ from $w(t)$ to $y(t)$ meets the constraint $\|H(s)\|_\infty \le \gamma$ where $\|H(s)\|_\infty = \sup_{\omega \in R} \sigma_{\max}[H(j\omega)]$ and $\sigma_{\max}[\cdot]$ denotes the largest singular value of $[\cdot]$; and γ is a given positive constant.

Remark 2: If the requirements C1 and C2 are met, the controlled manipulator system will have good robust performance, that is, good transient behavior and good disturbance rejection property in the presence of uncertainties. In next section, we will establish both the existence and the analytical expression of the expected controllers.

III. Robust H_∞ Control Design

To begin with, we present two lemmas as follows which will be essentially needed in the design of the robust H_∞ controller.

Lemma 1 [22]: Let a positive scalar $\varepsilon > 0$ and a positive-definite matrix $Q > 0$ be such that $\varepsilon S^T Q S < I$. Define $A_{cq} := A_c + qI$. Then we have

$$\begin{aligned}&(A_{cq} + \Delta A_c)^T Q (A_{cq} + \Delta A_c)\\ &\quad \le A_{cq}^T [Q + QS(\varepsilon^{-1} I - S^T Q S)^{-1} S^T Q] A_{cq}\\ &\qquad + \varepsilon^{-1} (N_1 + N_2 K)^T (N_1 + N_2 K).\end{aligned} \tag{14}$$

Lemma 2 [23]: Let $X \in \mathbb{R}^{m \times n}$ and $Y \in \mathbb{R}^{m \times p}$ $(m \le p)$. There exists a matrix V which satisfies simultaneously $Y = XV$ and $VV^T = I$ if and only if $XX^T = YY^T$.

We now show that, the circular pole and H_∞ performance constraints for all admissible parameter uncertainty can be guaranteed by the existence of a positive-definite solution to a modified algebraic Riccati equation. The corresponding result is stated in the following theorem which plays a key role for solving the problem RHCPPC.

Theorem 1: Let a positive constant $\gamma > 0$ and a circular region $D(-q, r)$ be given. Then the performance requirements C1 and C2 are satisfied if the following matrix inequality has a positive-definite solution $Q > 0$:

$$\begin{aligned}&(A_c + \Delta A_c)^T Q (A_c + \Delta A_c) + (q^2 - r^2) Q\\ &\quad + q\left[(A_c + \Delta A_c)^T Q + Q(A_c + \Delta A_c)\right.\\ &\qquad \left. + \gamma^{-2} Q D D^T Q + E E^T\right] \le 0.\end{aligned} \tag{15}$$

Proof: See the Appendix. ■

Remark 3: Theorem 1 implies that the H_∞ disturbance attenuation and the circular pole constraints are automatically enforced when a positive-definite solution to (15) is known to exist. Next, in Theorem 2, we will show that the uncertainties ΔA_c appearing in (15) can be removed with the help of Lemma 1.

Theorem 2: Let the desired disc $D(-q, r)$, the constant $\gamma > 0$ and the state feedback gain K be given. If there exist a positive scalar $\varepsilon > 0$ and a positive-definite matrix $Q > 0$ satisfying

$$\varepsilon S^T Q S < I \tag{16}$$

$$\begin{aligned}\Omega A_{cq} + \varepsilon^{-1} A_{cq}^T (N_1 + N_2 K)^T (N_1 + N_2 K) + q E^T E \\ = (r^2 - q\gamma^{-2} Q D D^T) Q\end{aligned} \tag{17}$$

where $\Omega := Q + QS(\varepsilon^{-1} I - S^T Q S)^{-1} S^T Q$, then the eigenvalues of the uncertain closed-loop system matrix $A_c + \Delta A_c$ are located within the desired disc $D(-q, r)$ and the H_∞ norm of the disturbance transfer matrix $H(s)$ from $w(t)$ to $y(t)$ meets the constraint $\|H(s)\|_\infty \le \gamma$.

Proof: See the Appendix. ∎

Remark 4: Theorem 1 provides the sufficient conditions under which the expected robust H_∞ circular pole constraints are achieved. It should be pointed out that, these sufficient conditions may be conservative which are produced primarily due to the utilization of (14). Fortunately, we can reduce the conservativeness in a matrix-norm sense by properly selecting the parameter ε (see [25] for details).

Now, we are in a position to discuss the design procedure of robust H_∞ controllers. We shall derive the conditions under which there exists a state feedback controller gain K such that the robust circular pole and H_∞ norm constraints can be achieved and the general expression of the desired feedback controller gain K.

Assume that (16) holds for a positive scalar $\varepsilon > 0$ and a positive-definite matrix $Q > 0$. After some algebraic manipulations, the (17) can be rearranged as follows:

$$\begin{aligned}&\left[(A + qI)^T \Omega B + \varepsilon^{-1} N_1^T N_2\right] K \\ &\quad + K^T \left[(A + qI)^T \Omega B + \varepsilon^{-1} N_1^T N_2\right]^T \\ &\quad + K^T \left(B^T \Omega B + \varepsilon^{-1} N_2^T N_2\right) K \\ &\quad + r^2 Q - q(\gamma^{-2} Q D D^T Q + E^T E) \\ &\quad - (A + qI)^T \Omega (A + qI) - \varepsilon^{-1} N_1^T N_1 = 0.\end{aligned} \tag{18}$$

Based on (18), our design problem can be converted into the following equivalent *Q-matrix assignment problem.*

- Find the necessary and sufficient conditions ("*assignability conditions*") for a positive-definite matrix Q under which there exists a controller gain K satisfying (18).
- If the controller gain K exists (i.e., the matrix $Q > 0$ is "*assignable*"), give the characterization of all expected controller gains in terms of the positive-definite matrix Q and some other free parameters.

We now focus on the Q-matrix assignment problem. Since $N_2^T N_2 > 0$, the matrix $B^T \Omega B + \varepsilon^{-1} N_2^T N_2$ is invertible, and (18), or (17), can be also rewritten as

$$\begin{aligned}&\Big[K^T \left(B^T \Omega B + \varepsilon^{-1} N_2^T N_2\right)^{1/2} \\ &\qquad + \left((A + qI)^T \Omega B + \varepsilon^{-1} N_1^T N_2\right) \\ &\qquad \cdot \left(B^T \Omega B + \varepsilon^{-1} N_2^T N_2\right)^{-1/2}\Big] \\ &\quad \cdot \Big[K^T \left(B^T \Omega B + \varepsilon^{-1} N_2^T N_2\right)^{1/2} \\ &\qquad + \left((A + qI)^T \Omega B + \varepsilon^{-1} N_1^T N_2\right) \\ &\qquad \cdot \left(B^T \Omega B + \varepsilon^{-1} N_2^T N_2\right)^{-1/2}\Big]^T \\ &= -r^2 Q + q(\gamma^{-2} Q D D^T Q + E^T E) + (A + qI)^T \Omega \\ &\quad \cdot (A + qI) + \varepsilon^{-1} N_1^T N_1 + \left[(A + qI)^T \Omega B + \varepsilon^{-1} N_1^T N_2\right] \\ &\quad \cdot \left(B^T \Omega B + \varepsilon^{-1} N_2^T N_2\right)^{-1} \left[(A + qI)^T \Omega B + \varepsilon^{-1} N_1^T N_2\right]^T.\end{aligned} \tag{19}$$

Observe that the left-hand side of (19) is nonnegative and $K \in \mathbb{R}^{n_u \times n_x}$. It is not difficult to find that there exists a feedback gain matrix K such that (19) holds if and only if Q satisfies the following matrix inequality:

$$\begin{aligned}\Sigma := &-r^2 Q + q(\gamma^{-2} Q D D^T Q + E^T E) + (A + qI)^T \Omega (A + qI) \\ &+ \varepsilon^{-1} N_1^T N_1 + \left[(A + qI)^T \Omega B + \varepsilon^{-1} N_1^T N_2\right] \\ &\cdot \left(B^T \Omega B + \varepsilon^{-1} N_2^T N_2\right)^{-1} \left[(A + qI)^T \Omega B + \varepsilon^{-1} N_1^T N_2\right]^T \\ &\ge 0\end{aligned} \tag{20}$$

and Σ is of rank which is not more than $\min(n_x, n_u)$. This gives the *assignability* conditions.

Furthermore, let matrix $T \in \mathbb{R}^{n_u \times n_x}$ be the square root of Σ, i.e., $TT^T = \Sigma$ (by Lemma 2, the square root satisfying $TT^T = \Sigma$ is not unique, and we can just choose one). If (20) holds, then (19) can be again expressed as follows:

$$\begin{aligned}&\Big[K^T \left(B^T \Omega B + \varepsilon^{-1} N_2^T N_2\right)^{1/2} \\ &\qquad + \left((A + qI)^T \Omega B + \varepsilon^{-1} N_1^T N_2\right) \\ &\qquad \cdot \left(B^T \Omega B + \varepsilon^{-1} N_2^T N_2\right)^{-1/2}\Big] \\ &\quad \cdot \Big[K^T \left(B^T \Omega B + \varepsilon^{-1} N_2^T N_2\right)^{1/2} \\ &\qquad + \left((A + qI)^T \Omega B + \varepsilon^{-1} N_1^T N_2\right) \\ &\qquad \cdot \left(B^T \Omega B + \varepsilon^{-1} N_2^T N_2\right)^{-1/2}\Big]^T = TT^T\end{aligned} \tag{21}$$

or equivalently (by Lemma 2)

$$\begin{aligned}K^T &\left(B^T \Omega B + \varepsilon^{-1} N_2^T N_2\right)^{1/2} + \left((A + qI)^T \Omega B + \varepsilon^{-1} N_1^T N_2\right) \\ &\cdot \left(B^T \Omega B + \varepsilon^{-1} N_2^T N_2\right)^{-1/2} = TV\end{aligned} \tag{22}$$

where $V \in \mathbb{R}^{n_u \times n_u}$ is an arbitrary orthogonal matrix. It follows immediately from (22) that the corresponding state feedback gain K can be obtained by

$$\begin{aligned}K = &\Big[TV \left(B^T \Omega B + \varepsilon^{-1} N_2^T N_2\right)^{-1/2} \\ &- \left((A + qI)^T \Omega B + \varepsilon^{-1} N_1^T N_2\right) \\ &\cdot \left(B^T \Omega B + \varepsilon^{-1} N_2^T N_2\right)^{-1}\Big]^T.\end{aligned} \tag{23}$$

Note that (23) provides a set of the desired controller gains in terms of the parameters Q, ε, V, where the parameter Q enters (23) indirectly via T and Ω.

Summing up, we conclude the above results in the following main theorem.

Theorem 3: Consider the uncertain linear continuous system (8). Given the desired circular pole region $D(-q, r)$ and the H_∞ norm bound constraint $\gamma > 0$ on the disturbance rejection attenuation. Let the notion Ω be defined as in Theorem 2, and Σ be defined by (20). If there exist positive scalar $\varepsilon > 0$ and a positive-definite matrix $Q > 0$ satisfying (16), (20), then with the state-feedback gain determined by (23), the expected performance requirements C1 and C2 can be achieved, i.e., for all admissible parameter uncertainties, the closed-loop poles are placed within the disc $D(-q, r)$ and the H_∞ norm of the disturbance transfer matrix $H(s)$ from $w(t)$ to $y(t)$ meets the constraint $\|H(s)\|_\infty \leq \gamma$.

Remark 5: Theorem 3 presents sufficient conditions for designing state feedback controllers which satisfy both the robust d-stability constraint and the robust H_∞ constraint, in terms of a simple linear matrix inequality (16) and a Riccati-like matrix inequality (20). When the uncertainties are absent (i.e., $M = N = 0$) and there are no constraints on the H_∞ norm of the disturbance transfer function (i.e., $\gamma = \infty,\ D = 0$), the condition in Theorem 1 will be both sufficient and necessary, and thus Theorem 3 actually parameterizes all state-feedback controllers which place the closed-loop poles within a specified disk for continuous-time systems. This means, Theorem 3 generalizes partial results of [11].

Remark 6: In practical applications, it is very desirable to directly solve the quadratic matrix inequality (QMI) (20) subject to the constraint (16), and then obtain the expected observer gain readily from (23). When working with the QMI, the local numerical searching algorithms suggested in [2], [9] are very effective for a relatively low-order model. A related discussion of the solving algorithms for QMIs can also be found in [18].

Remark 7: It can be seen from Theorem 3 that, unlike the algebraic Riccati equation method developed in [7], [8], [17], and [23], the present parameterized approach provides much explicit freedom in the design of state-feedback controllers because of the nonuniqueness in choosing the parameters Q, ε, V. This design freedom can be used to achieve other performance requirements, such as reliability against sensor failures, implementation accuracies and gain reduction, etc., which still require further investigation. Note that in Theorem 3, the addressed feedback control problem is converted into the solvability problem for a positive-definite matrix $Q > 0$ to satisfy two matrix inequalities. Therefore, in principle, if other system performance requirements can also be expressed in terms of linear/quadratic matrix inequalities, they can then be enforced into the current developed framework.

Remark 8: The state feedback control design problem is considered for linear uncertain systems with both circular pole and H_∞-norm constraints. A parameterization approach is developed, which enables us to obtain the set of state-feedback controllers in terms of some free parameters. It would be interesting to extend the present results to the output feedback case. Unfortunately, the parameterization method developed in this section cannot apply to the output feedback case in a straightforward way, which leaves us an important issue for future research.

IV. Simulation and Experimental Results

To study the performance of the proposed control algorithms, a simulation environment based on the software MATLAB/SIMULINK has been developed. For applying the developed robust H_∞ control approach, the dynamic model (8) parameter uncertainties is used. It is assumed that the desired trajectories are unknown, but bounded by

$$-30\,(\deg) \leq q_i \leq 30\,(\deg), \qquad \text{for } i = 1, 2, 3, 4.$$

We now consider the nonlinear dynamic model (7). Denote $\tilde{u} = [u_1 \cdots u_n]^T$, and it follows from (5) that $u = [\tilde{u}^T\ 0_{1\times n}]^T$. Accordingly, partition $B(x)$ as $B(x) = [B_{P1}(x)\ \ B_{P2}(x)]$. Then, (7) can be rewritten as

$$\dot{x}(t) = A(x)x(t) + B_{P1}(x)\tilde{u}(t). \tag{25}$$

As discussed in Section II, the nonlinear dynamic model (25) is linearized at the initial operating point, and the system parameters of (8), where B is replaced by B_{P1}, can be derived as follows:

$$A = \begin{bmatrix} 0_{8\times8} & I_{8\times8} \\ A_{21} & A_{22} \end{bmatrix}, \quad B_{P1} = \begin{bmatrix} 0_{8\times4} \\ B_2 \end{bmatrix}, \quad D = \begin{bmatrix} 0_{8\times4} \\ 0.1B_2 \end{bmatrix}$$

$$E = I_{16\times16}, \quad S = 0.1I_{16\times16}, \quad N_1 = 10\begin{bmatrix} 0_{8\times8} & 0_{8\times8} \\ \hat{N}_{11} & \hat{N}_{12} \end{bmatrix}$$

$$N_2 = 10\begin{bmatrix} 0_{8\times4} \\ \hat{N}_2 \end{bmatrix}$$

where

$$A_{21} = \begin{bmatrix} 0 & 0 & 0 & 0 & 1280 & 0 & -1 & 0 \\ 0 & 0 & 0 & 0 & 1364 & 11 & 276 & 41 \\ 0 & 0 & 0 & 0 & -219 & 33 & 26\,275 & 4 \\ 0 & 0 & 0 & 0 & -153 & 65 & 16\,088 & 59\,036 \\ 0 & 0 & 0 & 0 & -6226 & 24 & 597 & 94 \\ 0 & 0 & 0 & 0 & 15 & -108 & -176 & -482 \\ 0 & 0 & 0 & 0 & 208 & -100 & -64\,963 & 5100 \\ 0 & 0 & 0 & 0 & 7 & -56 & 1050 & -79\,852 \end{bmatrix}$$

$$A_{22} = \begin{bmatrix} -152 & -77 & 0 & 0 & 0 & 0 & 0 & 0 \\ -77 & -277 & 3 & -1 & 0 & 0 & 0 & 0 \\ 0 & 111 & -45 & -20 & 0 & 0 & 0 & 0 \\ 0 & -33 & -20 & -61 & 0 & 0 & 0 & 0 \\ 593 & 631 & -2 & -2 & 0 & 0 & 0 & 0 \\ 0 & 3 & 0 & 0 & 0 & 0 & 0 & 0 \\ 0 & 45 & 97 & 59 & 0 & 0 & 0 & 0 \\ 0 & 1 & 0 & 45 & 0 & 0 & 0 & 0 \end{bmatrix}$$

$$B_2 = \begin{bmatrix} 32.923 & 16.557 & -0.003 & -0.002 \\ 16.557 & 59.482 & -2.040 & 0.604 \\ -0.036 & -23.791 & 36.405 & 16.376 \\ -0.023 & 7.042 & 16.376 & 49.589 \\ -127.403 & -135.716 & 1.864 & 1.303 \\ 0.002 & -0.650 & -0.174 & -0.339 \\ 0.0319 & -9.595 & -78.257 & -47.917 \\ 0.001 & -0.293 & 0.002 & -36.200 \end{bmatrix}$$

$$\hat{N}_{11} = \begin{bmatrix} 0 & 0 & 0 & 0 & -0.058 & 0.083 & 0.033 & 0.509 \\ 0 & 0 & 0 & 0 & -23.029 & 56.282 & 76.303 & 235.236 \\ 0 & 0 & 0 & 0 & 26.469 & -36.220 & -2.563 & -273.340 \\ 0 & 0 & 0 & 0 & 1.921 & 58.151 & 144.609 & 125.741 \\ 0 & 0 & 0 & 0 & 37.869 & -53.998 & -21.080 & -330.640 \\ 0 & 0 & 0 & 0 & -33.142 & -2.832 & -136.734 & 320.840 \\ 0 & 0 & 0 & 0 & -7.360 & -77.784 & -211.548 & -138.259 \\ 0 & 0 & 0 & 0 & -23.767 & 37.576 & -28.464 & 356.041 \end{bmatrix}$$

$$\hat{N}_{12} = \begin{bmatrix} 0 & 0.016 & -0.001 & 0 & 0 & 0 & 0 & 0 \\ 0.016 & 3.363 & -0.173 & -0.172 & 0 & 0 & 0 & 0 \\ -0.019 & -7.609 & 0.193 & -0.019 & 0 & 0 & 0 & 0 \\ -0.001 & -7.506 & -0.019 & -0.363 & 0 & 0 & 0 & 0 \\ -0.027 & -10.661 & 0.279 & 0.020 & 0 & 0 & 0 & 0 \\ 0.024 & 15.992 & -0.235 & 0.378 & 0 & 0 & 0 & 0 \\ 0.005 & 12.334 & -0.009 & 0.534 & 0 & 0 & 0 & 0 \\ 0.017 & 7.828 & -0.207 & 0.096 & 0 & 0 & 0 & 0 \end{bmatrix}$$

$$\hat{N}_2 = \begin{bmatrix} 0 & -0.004 & 0.001 & 0 \\ -0.004 & -0.723 & 0.140 & 0.138 \\ 0.004 & 1.1636 & -0.156 & 0.015 \\ 0.001 & 1.614 & 0.015 & 0.293 \\ 0.006 & 2.292 & -0.226 & -0.016 \\ -0.005 & -3.438 & 0.190 & -0.305 \\ -0.001 & -2.651 & 0.008 & -0.431 \\ -0.004 & -1.683 & 0.168 & -0.077 \end{bmatrix}.$$

As stated in the problem description, the matrices, N_1, N_2, and S, which reflect the uncertainty intensity, are constructed to approximate the major linearization errors of the system (6), while the matrix D accounts for the disturbance input which results primarily from the actuator noises in implementation. The pole set of the open-loop system with no uncertainty is given as follows:

$$\begin{aligned} \{&0,\ 0,\ 0,\ 0,\ -299.62,\ -11.71 + 280.15i,\ -11.71 - 280.15i, \\ &-32.65 + 253.81i,\ -32.65 - 253.81i,\ -99.34, \\ &-20.11 + 10.60i,\ -20.11 - 10.60i,\ -0.14 + 10.30i, \\ &-0.14 - 10.30i,\ -7.28,\ 0.44\}. \end{aligned}$$

We can see from the last pole that the open-loop uncertainty-free system is unstable. We also notice that the distribution of the open-loop poles is quite scattered. Therefore, we consider the circular region $D(-70.1, 70)$ in the left-half complex plane.

TABLE III
DESIRED TRAJECTORIES FOR SIMULATION

	Joint 1 (deg)	Joint 2 (deg)	Joint 3 (deg)	Joint 4 (deg)
Trajectory A	$15\sin(0.2t)$	$15\sin(0.2t)$	$20\sin(0.4t)$	$20\sin(0.4t)$
Trajectory B	$20\sin(0.2t)$	$20\sin(0.2t)$	$30\sin(0.5t)$	$30\sin(0.5t)$

TABLE IV
SIMULATION RESULTS OF MULTIVARIABLE CONTROL

	LQR control	Robust H_∞ control
Trajectory A	Figs. 2 and 3	Figs. 4 and 5
Trajectory B	Unstable	Figs. 6 and 7

Our goal is to design the state feedback control law $\tilde{u} = Kx$ such that all closed-loop poles are assigned inside the prespecified circular region $D(-70.1, 70)$, and the H_∞ norm of the transfer function from the disturbance input to the system output satisfies $\|H(s)\|_\infty < 0.9$. The corresponding state feedback gain K can be obtained as

$$K = [\, K_{11} \quad K_{12} \,]$$

where we have K_{11} and K_{12}, shown at the bottom of the page.

For the closed-loop system, the performance objectives are well achieved, that is, the closed-loop poles are constrained to lie within the specified disc $D(-70.1, 70)$, and for all admissible parameter uncertainties, the maximum H_∞ norm of the disturbance transfer matrix $H(s)$ from $w(t)$ to $y(t)$ satisfies $\|H(s)\|_\infty = 0.5211 < 0.9$.

To make a comparison, a traditional LQR controller is designed where the weighting matrices are selected to be $Q = 0.01I$ and $R = 0.1I$.

In the simulation, the desired trajectories are selected as in Table III. The simulation results are shown in Table IV and from which we observe the following:

- Trajectory A is bounded in a relative small operating space including the initial point. Both simulated multivariable controllers are stable. The robust H_∞ controller performs better in tracking precision over the traditional LQR controller when the control energy is maintained at the same level.
- Trajectory B is bounded in a relative larger operating space. In this operating space, the LQR control is unstable. It is verified that the robust H_∞ controller performs better with respect to stability.

$$K_{11} = \begin{bmatrix} 46.1 & -22.5 & 25.9 & -2.56 & -1.1 & 3.2 & -33.7 & 174.7 \\ -17.4 & 33.6 & -22.7 & 3.4 & 15.6 & -0.9 & 50.9 & -152.6 \\ -8.6 & 5.6 & 28.0 & 9.7 & 10.0 & 0.8 & 691.0 & -1070.6 \\ -3.0 & 2.1 & 6.7 & 18.8 & -2.2 & 1.6 & 1.8 & 1710.9 \end{bmatrix}$$

$$K_{12} = \begin{bmatrix} 5.4 & 3.5 & 3.4 & 0.3 & 1.6 & 0.6 & 1.6 & -0.7 \\ -1.3 & -3.2 & -1.3 & 0.2 & 0.1 & 0.0 & -0.6 & 1.1 \\ 0.0 & 1.2 & 1.1 & 0.9 & 0.2 & 0.1 & 0.9 & 3.8 \\ 0.6 & 0.8 & 0.9 & -0.1 & 0.2 & 0.1 & 0.8 & -4.3 \end{bmatrix}.$$

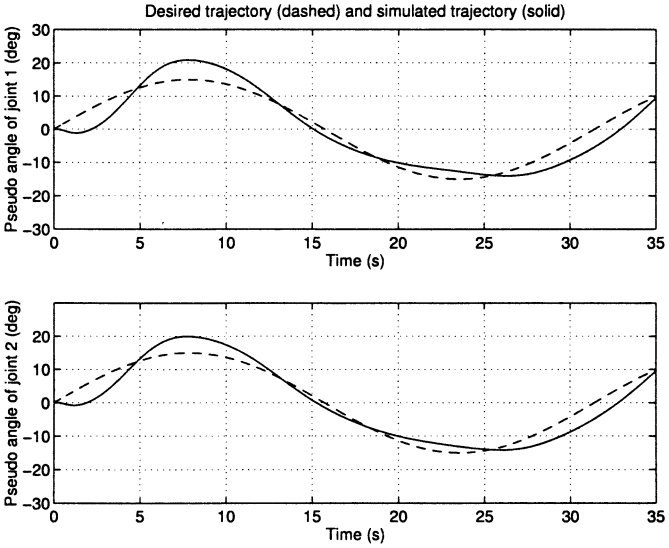

Fig. 2. Simulation results of LQR control. Tracking of trajectory A for joint 1 and joint 2.

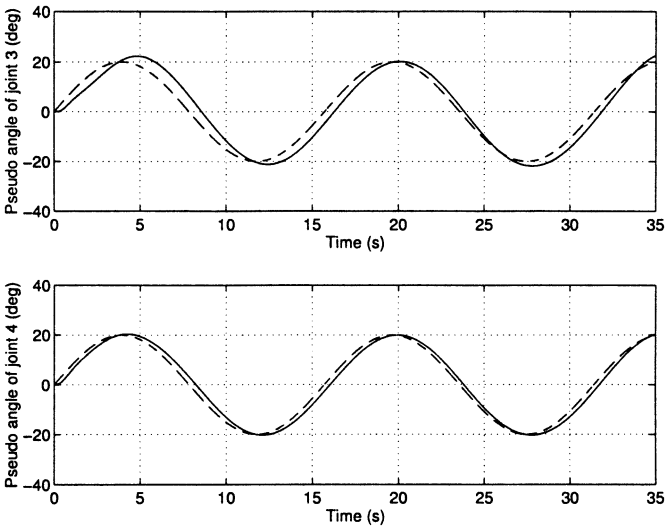

Fig. 3. Simulation results of LQR control. Tracking of trajectory A for joint 3 and joint 4.

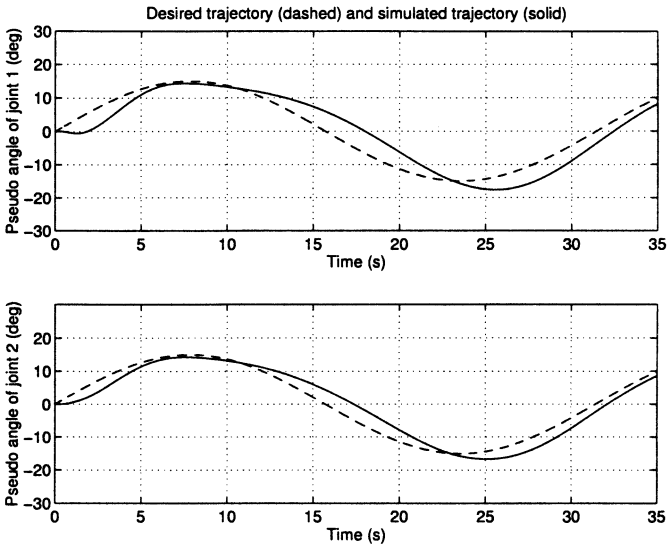

Fig. 4. Simulation results of robust H_∞ control. Tracking of trajectory A for joint 1 and joint 2.

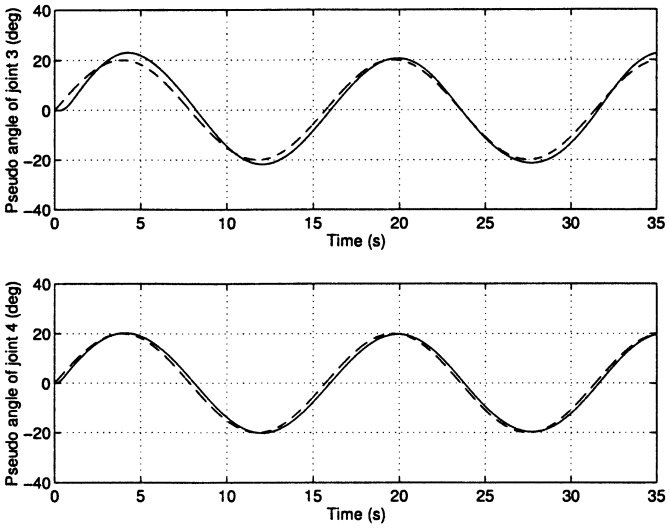

Fig. 5. Simulation results of robust H_∞ control. Tracking of trajectory A for joint 3 and joint 4.

It is apparent that the simulation results found in Figs. 2–7 verify theoretical analysis.

The experimental results are shown in Figs. 8 and 9 for end-effector tracking of a trajectory with 2.5-kg payload, respectively. Both LQR and robust H_∞ controller are used, respectively. The experimental results show that the robust H_∞ control performs better in tracking precision over the traditional LQR control.

V. Conclusion

The problem of robust H_∞ control for a multilink flexible manipulator has been addressed in this paper. A new approach to robust H_∞ control of multilink flexible manipulators has been presented using regional pole assignment. A multiobjective simultaneous realization problem has been introduced to the controller design such that the controlled manipulator system, for all admissible parameter uncertainties in the operating space, simultaneously satisfies both the prespecified H_∞ norm constraint on the transfer function from disturbance inputs to system outputs, and the prespecified circular pole constraint on the closed-loop system matrix. Simulation and experimental results have verified the theoretical analysis results and demonstrated the usefulness and applicability of the proposed approach.

Appendix

Proof of Theorem 1: Define $\Psi := (1/r)(A_c + \Delta A_c + qI)$. It is clear that the specified circular pole constraint $\sigma(A_c + \Delta A_c) \subset D(-q, r)$ is equivalent to the Schur stability of matrix Ψ, i.e., the eigenvalues of Ψ are all located inside the unit circle $D(0, 1)$. We know from the discrete-time Lyapunov stability theory that Ψ is Schur matrix if and only if there exists a positive-definite matrix Q meeting $Q - \Psi^T Q \Psi > 0$.

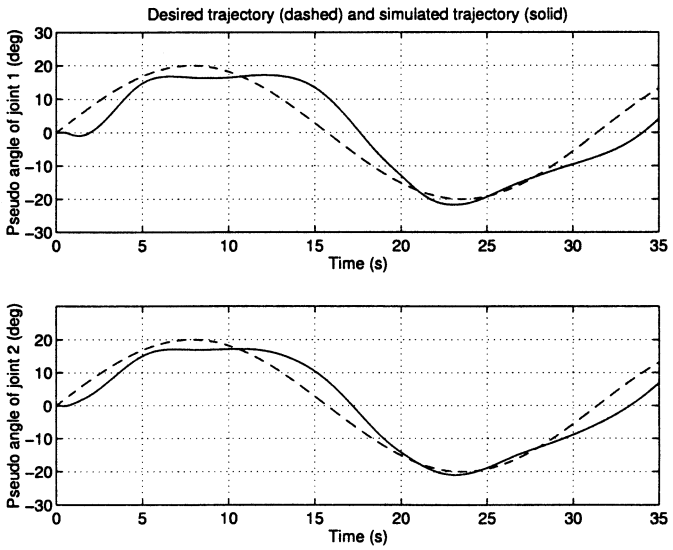

Fig. 6. Simulation results of robust H_∞ control. Tracking of trajectory B for joint 1 and joint 2.

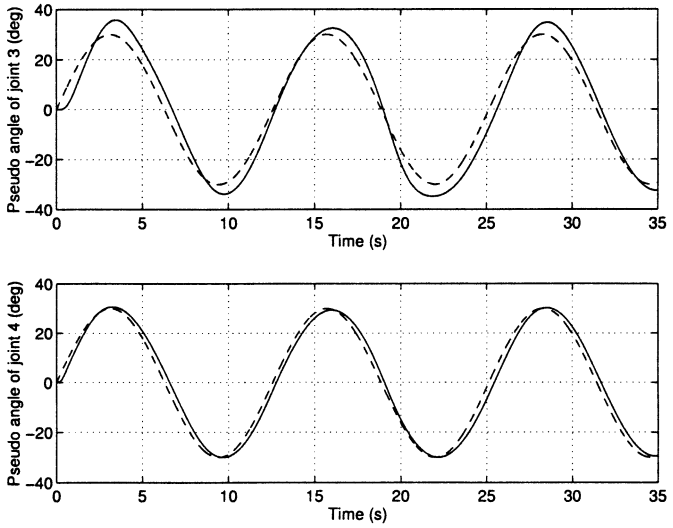

Fig. 7. Simulation results of robust H_∞ control. Tracking of trajectory B for joint 3 and joint 4.

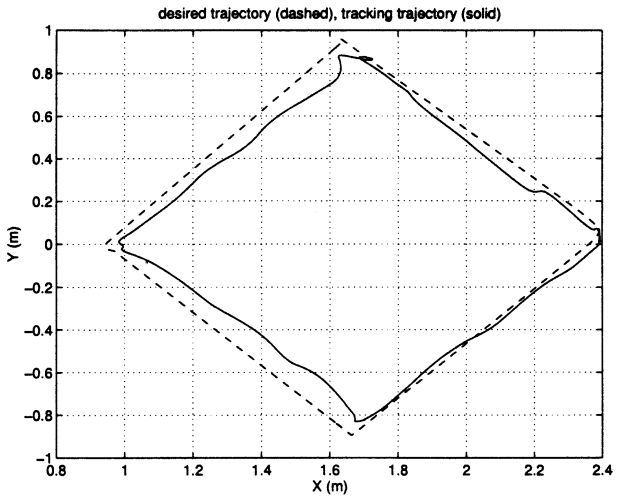

Fig. 8. LQR control. Endeffector tracking of a trajectory.

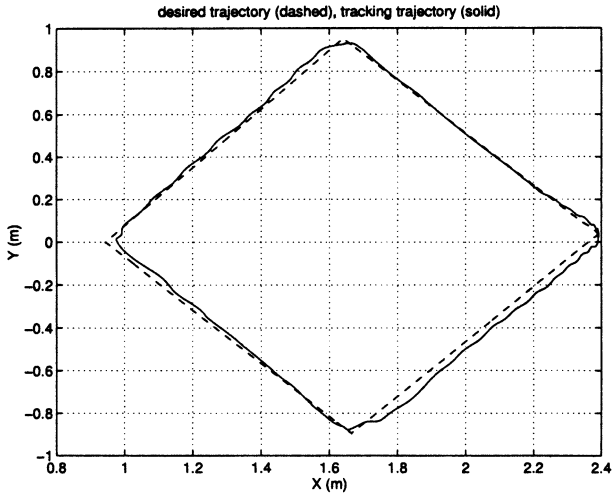

Fig. 9. Robust H_∞ control. End-effector tracking of a trajectory.

Since (15) holds, we can assume that there exists a matrix $P \geq 0$ (P may be dependent on the uncertain matrix F) such that

$$(A_c+\Delta A_c)^T Q(A_c+\Delta A_c)+(q^2-r^2)Q+q\left[(A_c+\Delta A_c)^T Q +Q(A_c+\Delta A_c)+\gamma^{-2}QDD^TQ+EE^T+P\right]=0. \quad (26)$$

It is not difficult to rewrite (26) as follows:

$$Q-\Psi^T Q\Psi=(q/r^2)(\gamma^{-2}QDD^TQ+E^TE+P)>0 \quad (27)$$

which indicates that the circular pole requirement C1 will be met.

Next, we can also rearrange (26) as follows:

$$(A_c+\Delta A_c)^T Q+Q(A_c+\Delta A_c)+\gamma^{-2}QDD^TQ+E^TE+\Sigma=0 \quad (28)$$

where

$$\Sigma=q^{-1}\left[(A_c+\Delta A_c)^T Q(A_c+\Delta A_c)+(q^2-r^2)Q\right]+P. \quad (29)$$

Since $\Sigma > 0$, the proof of $||H(s)||_\infty \leq \gamma$ can be completed by a standard manipulation of equation (28); for detail see [24, Lemma 1]. This completes the proof of Theorem 1.

Proof of Theorem 2: It follows from Lemma 1 that

$$\Theta := A_{cq}^T \Omega A_{cq}+\varepsilon^{-1}(N_1+N_2K)^T(N_1+N_2K) -(A_{cq}+\Delta A_c)^T Q(A_{cq}+\Delta A_c)\geq 0. \quad (30)$$

Then, by means of (30), we can rewrite (17) as follows:

$$(A_{cq}+\Delta A_c)^T Q(A_{cq}+\Delta A_c) = r^2Q-q(\gamma^{-2}QDD^TQ+E^TE+q^{-1}\Theta). \quad (31)$$

Furthermore, by defining $P := q^{-1}\Theta \geq 0$ and noting that $A_{cq}=A_c+qI$, we can continue to transform (31) as

$$q(A_c+\Delta A_c)^T Q+qQ(A_c+\Delta A_c)+(A_c+\Delta A_c)^T Q(A_c+\Delta A_c) +(q^2-r^2)Q+q(\gamma^{-2}QDD^TQ+E^TE+P)=0 \quad (32)$$

which has the same form as (26), then the proof of this theorem follows from Theorem 1 directly.

ACKNOWLEDGMENT

The authors are grateful to Prof. D. Prätzel-Wolters, University of Kaiserslautern, Germany, for useful suggestions.

REFERENCES

[1] H. Asada, Z. D. Ma, and H. Tokumaru, "Inverse dynamics of flexible robot arm: Modeling and computation for trajectory control," *ASME J. Dynamic Syst., Measurement, Contr.*, vol. 112, pp. 177–185, 1990.

[2] E. Beran and K. Grigoriadis, "A combined alternating projections and semidefinite programming algorithm for low-order control design," in *Proc. 13th IFAC World Congr.*, vol. C, San Francisco, CA, 1996, pp. 85–90.

[3] C. Chevallereau and Y. Aoustin, "Nonlinear control laws for a 2-link flexible robot: Comparison of applicability domains," in *Proc. IEEE Int. Conf. Robot. Automat.*, Nice, France, 1992, pp. 748–753.

[4] C. Canudas de Wit, B. Siciliano, and B. Georges, *Theory of Robot Control*. Berlin, Germany: Springer-Verlag, 1996.

[5] J. Daafouz, G. Garcia, and J. Bernussou, "Robust control of a flexible robot arm using the quadratic d-stability approach," *IEEE Trans. Contr. Syst. Technol.*, vol. 6, pp. 524–533, Sept. 1998.

[6] N. Fabritz, "Ein offenes Automatisierungssystem fuer einen mehrgliedrigen elastischen Manipulator," Ph.D. dissertation, Ruhr-University Bochum, Fortschrittsberichte VDI, VDI-Verlag, Duesseldorf, Germany, 1997.

[7] G. Garcia, "Quadratic guaranteed cost and disc pole location control for discrete-time uncertain systems," *Inst. Elect. Eng. Proc. Contr. Theory Applicat.*, vol. 144, pp. 545–548, 1997.

[8] G. Garcia and J. Bernussou, "Pole assignment for uncertain systems in a specified disk by state feedback," *IEEE Trans. Automat. Contr.*, vol. 40, pp. 184–190, Jan. 1995.

[9] J. C. Geromel, P. L. D. Peres, and S. R. Souza, "Output feedback stabilization of uncertain systems through a min/max problem," in *Prep. 12th IFAC World Congress*, vol. 6, Sydney, Australia, 1993, pp. 35–38.

[10] "Harmonic Drive," in *Hauptkatalog Antriebsmotoren* Limburg, Germany, 1990.

[11] W. M. Haddad and D. S. Bernstein, "Controller design with regional pole constraints," *IEEE Trans. Automat. Contr.*, vol. 37, pp. 54–69, Jan. 1992.

[12] D. W. C. Ho, J. Lam, and J. Xu, "Robust approximate pole assignment for second-order systems: Neural network computation," *J. Guidance, Contr., Dynamics*, vol. 21, no. 6, pp. 923–929, 1998.

[13] D. W. C. Ho, J. Lam, J. Xu, and H. K. Tam, "Neural computation for robust approximate pole assignment," *Neurocomput.*, vol. 25, pp. 191–211, 1999.

[14] P. T. Kotnic, S. Yurkovich, and U. Ozguner, "Acceleration feedback for control of a flexible manipulator arm," *J. Robotic Syst.*, vol. 5, no. 3, pp. 181–196, 1988.

[15] C. M. Pham, W. Khalil, and C. Chevallereau, "A nonlinear model-based control of flexible robots," *Robotica*, vol. 11, pp. 73–82, 1992.

[16] Z. Qu and D. M. Dawson, *Robust Tracking Control of Robot Manipulators*. New York: IEEE, 1996.

[17] S. O. Reza Moheimani and I. R. Petersen, "Quadratic guaranteed cost control with robust pole placement in a disk," *Proc. Inst. Elect. Eng. Contr. Theory Applicat.*, vol. 143, pp. 37–43, 1996.

[18] A. Saberi, P. Sannuti, and B. M. Chen, *H_2 Optimal Control*. London, U.K.: Prentice-Hall, 1995, Series in Systems and Control Engineering.

[19] M. Saeki, "H_∞ control with pole assignment in a specified disc," *Int. J. Contr.*, vol. 56, pp. 725–731, 1992.

[20] R. S. Smith, C. C. Chu, and J. L. Fanson, "The design of H_∞ controllers for an experimental flexible structure," *IEEE Trans. Contr. Syst. Technol.*, vol. 2, pp. 101–109, Jan. 1994.

[21] I. Y. Shung and M. Vidyasagar, "Control of a flexible robot arm with bounded input: Optimum step response," in *Proc. IEEE Conf. Decision Contr.*, 1986, pp. 1140–1144.

[22] Z. Wang, "Robust state estimation for perturbed systems with error variance and circular pole constraints: The discrete-time case," *Int. J. Contr.*, vol. 73, pp. 303–311, 2000.

[23] Z. Wang, G. Tang, and X. Chen, "Robust controller design for uncertain linear systems with circular pole constraints," *Int. J. Contr.*, vol. 65, pp. 1045–1054, 1996.

[24] J. C. Willems, "Least squares stationary optimal control and the algebraic Riccati equation," *IEEE Trans. Automat. Contr.*, vol. AC–16, pp. 621–634, Apr. 1971.

[25] L. Xie and Y. C. Soh, "Robust Kalman filtering for uncertain systems," *Syst. Contr. Lett.*, vol. 22, pp. 123–129, 1994.